JOURNAL OF CATALYSIS 147, 525–534 (1994)

CO Disproportionation on Silica-Supported Nickel and Nickel–Copper Catalysts

M. T. Tavares,* I. Alstrup,† C. A. Bernardo,* and J. R. Rostrup-Nielsen†

*Centro de Química Pura e Aplicada, Universidade do Minho, P-4719 Braga Codex, Portugal; and †Haldor Topsøe Research Laboratories, Nymøllevej 55, DK-2800 Lyngby, Denmark

Received June 14, 1993; revised November 26, 1993

The carbon formation/gasification equilibrium on silica-supported nickel and nickel–copper catalysts in CO + CO_2 gas mixtures and the steady state kinetics of carbon formation from CO on the same catalysts were studied in a thermogravimetric flow system. The equilibrium gas composition was found to be the same for the nickel and the nickel–copper catalysts except at the highest copper concentrations (≥25 at.%), where larger deviations from graphite equilibrium were found at the lowest temperature (673 K). The deviations at equilibrium of the free energy, ΔG_c, from the value calculated for graphite equilibrium were larger than found previously for carbon formation in CH_4 + H_2 gas mixtures. The steady-state kinetic results have been modelled by using a simple Langmuir model with one type of sites. In contrast to some previous studies of carbon formation from CO the present kinetic results are well described by a model in which the surface reaction of two CO molecules to form carbon and CO_2 is the rate-limiting step at temperatures below about 680 K and CO pressures in the range 15–50 kPa. At higher temperatures and pressures, the experimental rates fall below the model rates, probably due to diffusion limitations and to the partial coverage of the active surface by graphitic carbon. The conflict whereby a model with CO dissociation as the rate-limiting step gives a better description of the results of some previous kinetic studies of carbon formation from CO is suggested to be resolved by assuming that the latter model is valid when the CO pressure is low or when the gas contains CO_2.

1. INTRODUCTION

Carbon formation on transition metal catalysts from the decomposition of hydrocarbons or carbon monoxide has been studied extensively for many years. One major reason for this interest in carbon formation is that it can cause very important operational problems in a number of industrial catalytic processes (1). Under usual conditions, long carbon filaments grow out of the catalytic metal particles without blocking the processes responsible for this growth. In this way accumulation of huge amounts of carbon in and on the catalyst pellets is possible which can create very severe problems in the reactor.

One way to reduce the risk of carbon formation is to add to the surface an agent which poisons the carbon formation reaction more than the desired process. In industrial steam reforming this can be achieved by using sulfur as the selective poisoning agent (2). A similar effect might be obtained by adding copper to the nickel surface (3).

The mechanism of the catalytic growth of carbon filaments has been discussed for more than 20 years and is still lively debated (4–14). Dent and Cobb (4) concluded from their studies of the decomposition of CO and CH_4 on a nickel catalyst that both processes had smaller equilibrium constants than those based on graphite data. Rostrup-Nielsen (5) also found deviations from graphite equilibrium for CO and CH_4 on a large number of nickel catalysts and suggested that the deviations could be explained by the extra energy required for the formation of the surface and of the defects of the filaments. Lobo *et al.* (6) and Baker *et al.* (7) explained, independently, carbon filament growth by a model according to which carbon atoms formed by decomposition of molecules on the metal particle surface migrate through the particle and segregate out into the carbon filament.

Although this model has been questioned by Manning *et al.* (8) and by Geus and co-workers (9–11) it is still generally considered to provide a realistic description of the mechanism of the steady growth of carbon filaments. Alstrup (12) pointed out that most of the objections against the model can be met by adding a proper description of the induction period and by improving the estimate of the energy of filament formation.

Bernardo *et al.* (3) showed that the deviation from graphite equilibrium of the carbon formation/gasification equilibrium in CH_4 + H_2 gas mixtures is the same for silica-supported Ni–Cu catalysts as for monometallic Ni catalysts, except at very high Cu concentrations (>50 at.% Cu) in the metal particles.

A number of studies of carbon formation have provided information about the kinetics of the process. Baker *et al.* (7) showed that the activation energy of the rate of

0021-9517/94 $6.00

growth of filamentous carbon correlated for Ni, Fe, Co, and Cr with the activation energy of carbon diffusion in the metal and suggested that the diffusion of carbon through the metal particles is rate-limiting for filament growth. On the other hand, Grabke (13) showed long ago that kinetic measurements of carbon deposition on α- and γ-iron surfaces exposed to $CH_4 + H_2$ gas mixtures could be explained quantitatively by assuming a mechanism based on a stepwise dehydrogenation of surface species after chemisorption of the methane molecules and with the dehydrogenation of methyl species as the rate-limiting step. Lázár *et al.* (14) found, however, that this model could not explain the observed kinetics when iron is replaced by nickel. Recently, Alstrup and Tavares (15) showed that kinetic data for carbon formation on a Ni/SiO_2 catalyst from $CH_4 + H_2$ gas mixtures can be explained by a model similar to the Grabke model but with the dissociative chemisorption of CH_4 as the rate-limiting step. The same type of model can also explain the observed rates for a $Ni_{0.99}Cu_{0.01}/SiO_2$ catalyst, while it can only explain the rates for a $Ni_{0.9}Cu_{0.1}/SiO_2$ catalyst at low carbon activities. At higher carbon activities the observed rates were much higher than predicted of the model. Alstrup and Tavares (16) were also able to construct a microkinetic model based on experimental and theoretical values for the binding and vibrational energies of the surface species involved. However, the modeling indicated that the assumption of a single rate-limiting step is not realistic, but that both the chemisorption step and the first dehydrogenation step are far from equilibrium.

Several authors (11, 17–19) have apparently assumed that the rate of carbon formation at constant temperature is solely a function of the carbon activity, a_c, of the gas, as they have presented rates plotted versus a_c.

The carbon activity a_c of a $CH_4 + H_2$ gas mixture is defined by

$$a_c = K_{p1} P_{CH_4} / P_{H_2}^2, \qquad [1]$$

where K_{p1} is the equilibrium constant of the reaction

$$CH_4 \rightleftharpoons C(\text{graphite}) + 2H_2.$$

The carbon activity a_c of a $CO + CO_2$ gas mixture is defined by

$$a_c = K_{p2} P_{CO}^2 / P_{CO_2}, \qquad [2]$$

where K_{p2} is the equilibrium constant of the Boudouard reaction

$$CO + CO \rightleftharpoons C(\text{graphite}) + CO_2.$$

Audier and Coulon (17) studied carbon formation from $CH_4 + H_2$ as well as from $CO + CO_2$ gas mixtures on an iron–nickel catalyst and plotted the rates versus a_c. The plots showed that the rates depend linearly on a_c in both cases and with the same slopes. On the other hand, and in agreement with the fact that a Grabke type model describes well the kinetic data of Alstrup and Tavares (15), a plot of rates versus a_c in Ref. (15) corresponded to strongly scattered points which could not fit any reasonable curve.

Few studies have provided sufficient data for testing kinetic models for carbon formation from CO on nickel. Tøttrup (20) measured the steady state rates of carbon formation on an alumina-supported nickel catalyst in $CO + CO_2$ gas mixtures for a range of CO and CO_2 partial pressures at 573, 593, and 613 K. The results were in good agreement with a kinetic model comprising a CO chemisorption step, dissociation of chemisorbed CO, formation of CO_2 by reaction between chemisorbed CO and O and desorption of CO_2. By assuming that the dissociation of CO is rate-limiting, Tøttrup derived expression [3] for the rate r_c of carbon formation

$$r_c = k \frac{P_{CO}}{[1 + K_A P_{CO} + K_B (P_{CO_2}/P_{CO})]^2} \qquad [3]$$

where k is the product of the rate constant for the rate-limiting step and K_A, where K_A is the equilibrium constant of the chemisorption of CO. K_B is a combination of equilibrium constants. By varying these constants Tøttrup obtained reasonable agreement with the experimental data (20). Rosei *et al.* (21) studied CO decomposition on a Ni(110) single crystal surface in the temperature range 473–673 K at CO pressures between 1.3×10^{-4} and 4.0×10^{-3} Pa. They tested three kinetic models on their kinetic data. The first model is the same as the model used by Tøttrup (20) described above. The second model is based on the assumption that the rate-limiting step is a surface reaction between two chemisorbed CO molecules giving carbon and CO_2 on the surface. The third model is similar to the second but only one of the two CO molecules reacting with each other to form carbon and CO_2 is chemisorbed before the reaction step; i.e., the model corresponds to an Eley–Rideal mechanism. However, it is not possible to distinguish between models 2 and 3 by fitting the models to the experimental rates because their rate expressions have the same structure. Rosei *et al.* (21) concluded that only the first model could be fitted to the experimental results. Kuijpers *et al.* (22) studied, through magnetic measurements, the differences between the carbon formed from CO and from CH_4 on a Ni/SiO_2 catalyst at 500 K. They also reported a few kinetic results for the decomposition of CO, e.g. that the rate is independent of

the CO pressure at the conditions used. They observed that the rate of reaction of surface oxygen with chemisorbed CO was of the same order of magnitude as the rate of carbon formation from CO and suggested that the above mentioned model 1 applies but with the surface reaction between chemisorbed CO and O as the rate-limiting step. Sakai *et al.* (23) measured rates as functions of time of carbon formation by decomposition of CO at temperatures in the range 773–1023 K and at CO pressures in the range 0.06–1.0 atm. They obtained good fits to the experimental results using the second model described by Rosei *et al.* (21), i.e., by assuming that carbon is formed by the surface reaction between two CO molecules.

With the aim of contributing to the understanding of the mechanism and kinetics of carbon formation on nickel and nickel–copper catalysts by decomposition of carbon monoxide, the present paper presents studies of rates of carbon formation and gasification on silica-supported nickel and nickel–copper catalysts in CO + CO_2 gas mixtures with compositions close to equilibrium, as well as kinetic studies of carbon formation on the nickel catalyst and on one of the nickel–copper catalysts for a range of temperatures and CO pressures.

2. EXPERIMENTAL

2.1. Preparation of Catalysts

The Ni/SiO_2 and $NiCu/SiO_2$ catalysts were prepared by "dry" impregnation with 20 wt% metal phase and NiCu catalysts with Cu:(Ni + Cu) ratios of 0.01, 0.1, 0.25, and 0.5. The required amounts of nickel and copper nitrates were dissolved in a volume of water equal to the measured pore volume of the support material (Cab-O-Sil H_5). The solution and the support material were mixed, dried at room temperature, and calcined at 773 K for 3 h. The resulting powder was mixed in a mortar with a plasticizer (Melhorel Dow A_4C) and water. The final paste was extruded in small, cylindrical pellets with 4 mm diameter and 4 mm length. The pellets were calcined for 2 h at 873 K and prereduced at 773 K in H_2 for 44 h.

2.2. Characterization of Catalysts

The samples were characterized by hydrogen chemisorption, nitrogen adsorption, X-ray diffraction and by transmission and scanning electron microscopy. The composition of the catalysts was checked by elemental chemical analysis.

2.3. Reactor System and Reactants

The determinations of the rates of carbon formation were based on monitoring the weight variations of the catalyst samples under reaction conditions by means of a C.I. Electronics MKIIB microbalance. The microbalance has a capacity of 1 g and a sensitivity of 1 μg. The sample was suspended in a silica basket inside a flow reactor with associated furnace and flow and temperature controllers. A thermocouple was placed inside the reactor, close to the sample, in the flat part of the furnace temperature profile. The temperature of the reactor wall was measured by another thermocouple at the same level as the sample.

The gases used (CO, CO_2, H_2, and N_2) were of high purity (>99.95%). The hydrogen was cleaned further by passing through a Cu furnace, held at 523 K, and mixed with the other reactant in a silica gel and in a 4A molecular sieve trap.

2.4. Experimental Conditions

The system was cleaned by a N_2 flow before each run. All samples were reduced for 1 h in a hydrogen flow of 6.7×10^{-5} mol · s^{-1} after which the temperature of the sample was adjusted to the selected reaction temperature and the system was cleaned again by a flow of N_2. A total flow of 2.98×10^{-4} mol · s^{-1} of reactants was admitted to the reactor when the temperature had stabilized. The balance was made with nitrogen. The rates of carbon deposition were determined from the slopes of the curves drawn by the microbalance recorder. A fresh sample was used in each isothermal run as well as in equilibrium determinations. A few runs were made in which a sample went through a few cycles of carbon deposition–gasification–deposition, etc.

A few runs were made to investigate whether the temperature measured just outside the sample was different from the sample temperature. The sample, a Ni/SiO_2 catalyst, was suspended, attached to a thermocouple in the center of the sample. The tests were made at the typical conversions used in the experiments, 0.3–0.6%, and at temperatures between 650 and 715 K. The difference of the temperatures measured by the two thermocouples was in all cases in the range 1–3 K, i.e., within the uncertainty of the measurements.

3. RESULTS

3.1. Catalysts

The fresh Ni/SiO_2 and $NiCu/SiO_2$ catalysts had a BET area of 250 m^2 g^{-1}, which after carbon deposition was reduced to about 150 m^2 g^{-1}. The average pore radius changed from 6.7 nm for the fresh catalyst to ca. 9 nm after deposition. The width of the X-ray diffraction peaks indicated an average diameter of the metal crystallites of about 25 nm, with a slightly lower value for the $Ni_{0.99}Cu_{0.01}/SiO_2$ catalyst than for the other ones. The total hydrogen uptake and the chemisorption of "strongly held" hydrogen (3) was determined for the fresh Ni/SiO_2 and $Ni_{0.9}Cu_{0.1}/SiO_2$ catalysts at 298 K and at hydrogen

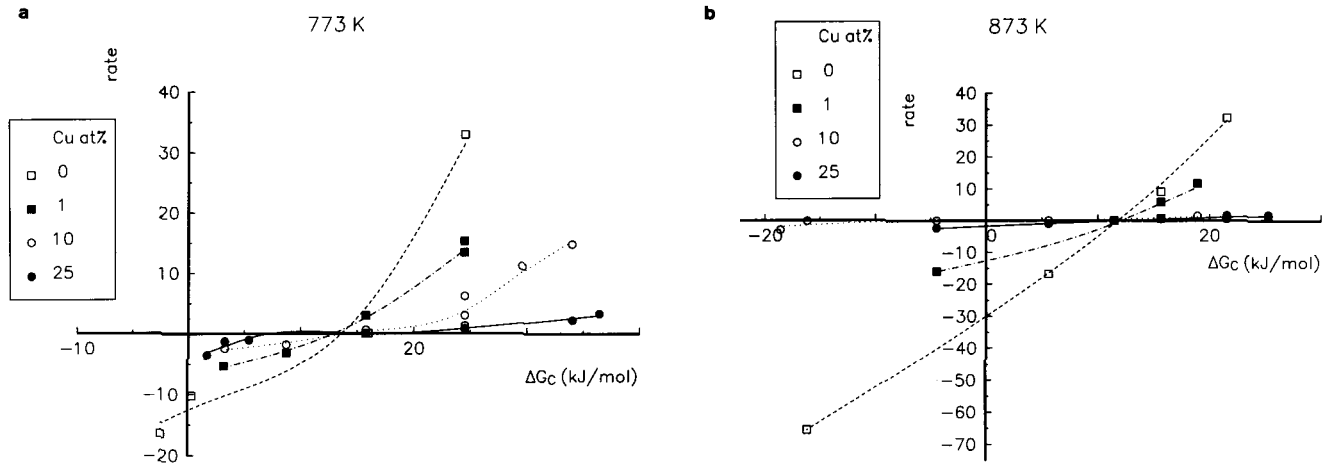

FIG. 1. Carbon deposition and gasification rates close to equilibrium plotted versus the deviation, ΔG_C, of the free energy of the CO + CO_2 gas mixtures from graphite equilibrium gas; (a) 773 K; (b) 873 K. The lines serve only to guide the eyes.

pressures in the range 5–15 kPa. The results for the total hydrogen uptake for the two catalysts were 150 and 111 μmol H_2/g_{cat}, respectively. The results for the strongly adsorbed hydrogen were 87 and 48 μmol H_2/g_{cat}, respectively. The 45% drop in the capacity of strongly chemisorbed hydrogen when going from the Ni catalyst to the NiCu catalyst indicates that some surface segregation of copper has taken place, but it also indicates that the surface copper enrichment was not as strong as found previously (3) for samples prepared in almost the same way, where an 80% drop was observed.

3.2. *Near Equilibrium Results*

Carbon deposition rates and gasification rates obtained at 773 K and 873 K, close to gas-carbon equilibrium for four catalysts with different Ni : Cu ratios are plotted versus ΔG_C *in Figs. 1a and 1b, respectively. Similar results* were also obtained at 673 and 973 K. As mentioned above, it is not to be expected that the rate at constant temperature depends solely on the carbon activity, a_C, of the gas (or on the carbon potential, $\Delta G_C = RT \ln a_C$, i.e., the deviation of the free energy of the gas from the one corresponding to the graphite equilibrium). Two different gas compositions with the same a_C (and ΔG_C) value and at the same temperature may, as mentioned above, give different carbon deposition or gasification rates, but the change from carbon deposition to gasification will take place at one and the same a_C (and ΔG_C) value irrespective of differences in the partial pressures. The results in Fig. 1 are used only for the determination and discussion of the deviation of the deposition/gasification equilibrium from the graphite equilibrium and in this case it is practical to use ΔG_C as the independent variable in the plots of Fig. 1. This is justified because ΔG_C is varied by changing only one of the partial pressures. In the carbon deposition region only the CO pressure and in the gasification region only the CO_2 pressure are varied. The results show that by gradually changing ΔG_C from a value above 20 kJ/mol to below 10 kJ/mol a continuous change from carbon deposition to gasification is observed in most cases. The value of ΔG_C where the change from deposition to gasification takes place is approximately the same for all the samples. For the $Ni_{0.9}Cu_{0.1}/SiO_2$ and the $Ni_{0.75}Cu_{0.25}/SiO_2$ sample at 873 K a continuous change from deposition to gasification could not be observed because the limited sensitivity of the microbalance prevented observations of measurable gasification rates in a broad ΔG_C range. The equilibrium ΔG_C values obtained from the plots are shown in Table 1. For the samples with Cu concentrations below 25 at.% the equilibrium ΔG_C is independent of the Cu content. To initiate carbon formation on a fresh catalyst it turned out to be necessary to increase ΔG_C of the gas to a value significantly higher than the equilibrium value. The start values observed are shown in Table 2. In a few experiments the sample went through a number of carbon deposition and gasification cycles. During these cyclings each change from decomposition to gasification and vice versa took place at the same ΔG_C value.

TABLE 1

ΔG_C (kJ/mol), Free Energy Deviation from Graphite Equilibrium at Carbon Formation Equilibrium

	Ni : Cu				
T (K)	1 : 0	99 : 1	9 : 1	75 : 25	20 : 80
673	20.2	20.2	20–27	36–56	36–59
773	15.8	15.8	15.8	9–15	—
873	11.5	11.5	4.5–5.6	9–15	—

TABLE 2

ΔG_C (kJ/mol), Free Energy Deviation from Graphite Equilibrium at Start of Carbon Formation

	Ni : Cu				
T (K)	1 : 0	99 : 1	9 : 1	75 : 25	20 : 80
673	27.1	36.1	23.8	60.3	59.0
773	24.5	24.5	15.8	36.4	—
873	21.5	15.6	15.6	25.3	—
973	14.4	4.4	1.4	—	—

3.3. Kinetic Results

The carbon deposition rates obtained for Ni/SiO_2 at 613, 653, 673, 693, and 713 K, for CO pressures in the range 10–30 kPa and, at 653 K, also for CO pressures in the range 30–80 kPa are shown in Fig. 2. Similar results are plotted in Fig. 3 for $Ni_{0.9}Cu_{0.1}/SiO_2$ at the same conditions. The results for Ni/SiO_2 in the CO pressure range 10–30 kPa are also plotted versus $1000/T$ (T = temperature in Kelvin) in Fig. 4, together with additional results at P_{CO} = 20 kPa. Similar plots are shown for $Ni_{0.9}Cu_{0.1}/SiO_2$ in Fig. 5. The lines in Figs. 2–5 show the results of kinetic modelling discussed in Section 4.2 below.

4. DISCUSSION

4.1. Near Equilibrium Results

The present results show that the same CO + CO_2 gas composition corresponds to equilibrium between the gas and the carbon formed on the nickel and on the nickel–copper catalysts with the exception of the catalyst

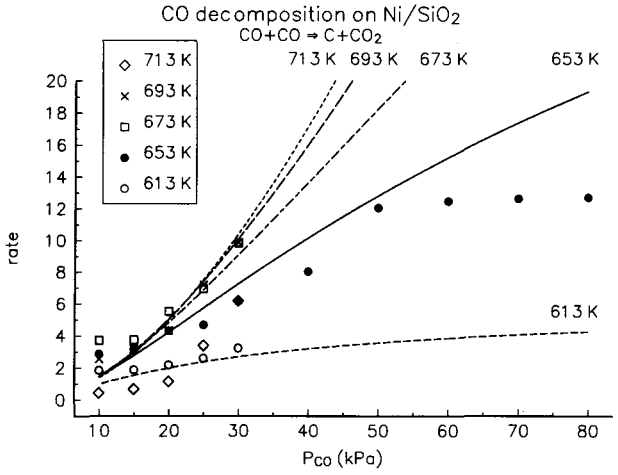

FIG. 2. Carbon deposition rates on the Ni/SiO_2 catalyst at CO pressures of 10, 15, 20, 25, and 30 kPa and at temperatures 613, 653, 673, and 713 K and in addition at CO pressures 40, 50, 60, 70, and 80 kPa at 653 K. The lines are calculated using the kinetic model 2.

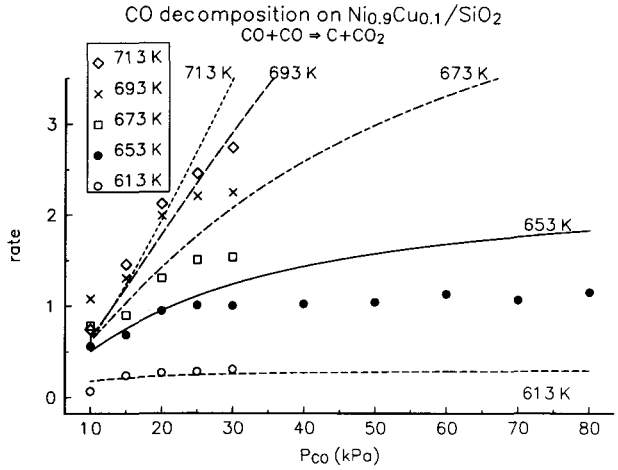

FIG. 3. Carbon deposition rates on the $Ni_{0.9}Cu_{0.1}/SiO_2$ catalyst at CO pressures of 10, 15, 20, 25, and 30 kPa and at temperatures 613, 653, 673, 693, and 713 K and in addition at CO pressures 40, 50, 60, 70, and 80 kPa at 653 K. The lines are calculated using the kinetic model 2.

with the highest copper content. Similar results were obtained by Bernardo *et al.* (3) for the carbon equilibrium on nickel and nickel–copper catalysts in CH_4 + H_2 gas mixtures. This indicates that the same type of carbon is formed on the nickel and on the nickel–copper catalysts. The studies of the rates close to equilibrium also show that when the carbon potential of the gas is gradually reduced, the process changes continuously from carbon deposition through equilibrium to gasification demonstrating the reversibility of the processes. The reversibility of the carbon formation and gasification on nickel catalysts in CH_4 + H_2 mixtures was similarly demonstrated previously in Ref. (12). The generally accepted model explaining carbon filament growth on transition metals is

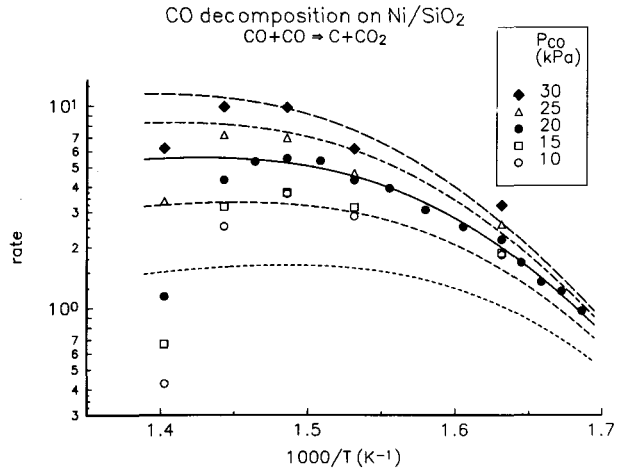

FIG. 4. Arrhenius plots of carbon deposition rates for the Ni/SiO_2 catalyst at CO pressures of 10, 15, 20, 25, and 30 kPa. The lines are calculated using the kinetic model 2.

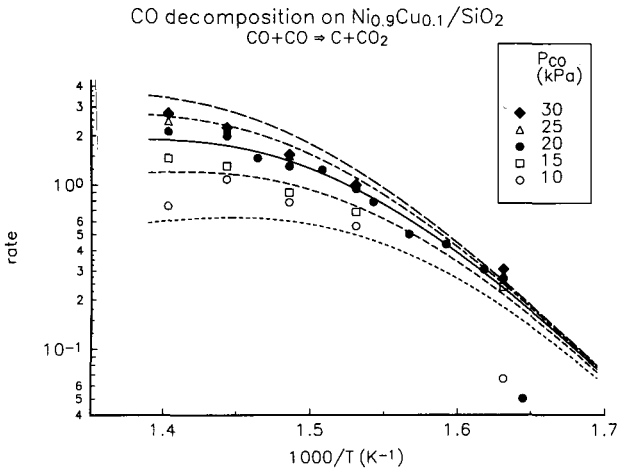

FIG. 5. Arrhenius plots of carbon deposition rates for the $Ni_{0.9}Cu_{0.1}/SiO_2$ catalyst at CO pressures of 10, 15, 20, 25, and 30 kPa. The lines are calculated using the kinetic model 2.

expected to be valid both for hydrocarbons and for CO-containing gases. This means that we would expect that the carbon activity of the gas is the same at carbon formation equilibrium independent of the nature of the gas. However, the comparison in Table 3 between the present equilibrium results and similar results obtained by Bernardo *et al.* (3), for carbon formation from $CH_4 + H_2$ on similar catalysts prepared and activated in the same way, shows that the carbon activity, a_C, and the carbon potential, ΔG_C, at equilibrium are higher for carbon formation from $CO + CO_2$ than from $CH_4 + H_2$ gas mixtures. An analogous difference between the carbon activities of the two gases at equilibrium is seen in the results of Rostrup-Nielsen (5). The reversibility of the carbon formation process implies that the carbon potential of the gas at equilibrium is determined by the energy of formation of the carbon. This means that the difference in the equilibrium carbon potentials for the two gases is either due to systematic errors in one or both of the equilibrium constants for the gases in equilibrium with graphite or to different energies of formation of the carbon formed in the two gases. The equilibrium constants used in the present work are calculated using the computer methods developed by Kjær (24). The values obtained are close to the values which can be calculated using published thermochemical data, e.g. by Turkdogan (25). In Ref. (25) the uncertainty of the free energies of the two carbon formation reactions considered here are estimated to be less than ±9 kJ/mol. It is thus unlikely that the observed differences in Table 3 are solely due to errors in the equilibrium constants used in the calculation of the ΔG_C values. It has been shown by Tracz *et al.* (26) that the morphology of the carbon formed on nickel catalysts in a reforming gas depends on temperature and on the catalyst support. On the other hand, studies of the influence of the gas composition on the morphology of the carbon formed have not been reported. Preliminary electron microscopic studies at the Haldor Topsøe Research Laboratories (27) indicate, however, that at the temperatures of the present experiments, only filaments are seen after carbon formation in $CH_4 + H_2$ and the nickel particles have regular crystalline shapes. After carbon formation in $CO + CO_2$, the nickel particles look irregular and a significant part of the carbon is of an encapsulating type with many imperfections. Thus, we may tentatively suggest that the differences in the carbon equilibrium for nickel catalysts in $CH_4 + H_2$ and $CO + CO_2$ reflect differences in the type and perfection of the carbon formed. It is tempting to try to obtain information about the energy and perfection of the carbon formed by using the temperature dependence of ΔG_C, the deviation from the graphite value of the free energy of formation of the carbon phase, to calculate an enthalphy, ΔH_C, and an entropy, ΔS_C, component. Such a determination is, however, beset with difficulties because of the large uncertainties of the ΔG_C values. Nevertheless, it may be significant that from the carbon equilibrium results in $CH_4 + H_2$ of Bernardo *et al.* (3), a ΔS_C value close to zero is obtained, while the present results give $\Delta S_C \approx 44$ J mol^{-1} K^{-1}.

TABLE 3

ΔG_C (kJ/mol), Free Energy Deviation from Graphite Equilibrium at Carbon Formation Equilibrium

T (K)	ex-CO p.w.[a]	ex-CH_4 Ref. (3)	ex-CO Ref. (5)	ex-CH_4 Ref. (5)
673	20.2	5.2	—	8
773	15.8	5.1	9	3
873	11.5	5.2	4	3

[a] Present work.

4.2. Kinetic Models

Several authors (11, 17–19) have indicated that the rate of carbon formation from CO and CH_4 containing gases is at constant temperature solely a function of the carbon activity, a_C, of the gas. Other authors (21) have suggested three different kinetic models to explain observed kinetic results for carbon formation on nickel catalysts from decomposition of CO. The validity of one of these three models implies that at constant temperature a_C does not solely determine the rate of carbon formation.

The kinetic model 1, which is claimed by Tøttrup (20) and by Rosei et al. (21) to give a good description of their results, is based on the following steps

$$CO + * \rightleftharpoons CO* \quad [4]$$

$$CO* + * \rightarrow C* + O* \quad [5]$$

$$CO* + O* \rightleftharpoons CO_2* + * \quad [6]$$

$$CO_2* \rightleftharpoons CO_2 + *, \quad [7]$$

where the asterisk (*) signifies a surface site and C*, O*, CO*, and CO_2* are chemisorbed species. It is assumed that the dissociation of chemisorbed CO, step 5, is rate-limiting and that the other steps are in quasi-equilibrium. It is further assumed that the Langmuir prescription is valid, i.e., that only one type of sites is present on the surface and that each of the surface species can occupy one and only one of the sites. With these assumptions it is then easy to derive the rate expression [3], if it is assumed, in addition, that the coverages of CO_2 and C are negligible and that the reaction takes places at conditions far from equilibrium. In expression [3] $k = k_5K_4$ and $K_A = K_4$, where k_5 is the forward rate constant of step 5 and K_4 is the equilibrium constant of step 4. Such a simple model of the surface is a rather crude approximation considering that the different adsorbates may bind to different types of sites, that interactions between the adsorbates may influence the reactions and that local reconstructions may be induced by the adsorbates. However, experience shows that this type of model can in many cases give an accurate description of similar steady-state kinetic results. A recent example is the accurate description of the rate of carbon formation from $CH_4 + H_2$ on Ni/SiO_2 and $NiCu/SiO_2$ catalysts (15, 16).

Sakai et al. (23) explained their kinetic results by replacing the steps (5) and (6) above by the rate-limiting step:

$$CO* + CO* \rightarrow C* + CO_2*. \quad [8]$$

With the same assumptions as above this model gives the following expression for the rate of carbon formation

$$r_C = k\frac{P_{CO}^2}{[1 + K_AP_{CO}]^2}, \quad [9]$$

where k is the product of the rate constant of the rate-limiting step and of $K_A^2 \cdot K_A$ is, as before, the equilibrium constant of the chemisorption of CO. Whether the experimental data can be described well by expression [3] or [9] is most easly tested by transforming them into linearized forms

$$\sqrt{\frac{P_{CO}}{r_C}} = \frac{1}{\sqrt{k}}\left(1 + K_AP_{CO} + K_B\frac{P_{CO_2}}{P_{CO}}\right) \quad [10]$$

and

$$\frac{P_{CO}}{\sqrt{r_C}} = \frac{1}{\sqrt{k}}(1 + K_AP_{CO}) \quad [11]$$

corresponding to (3) and (9), respectively. Model 3 leads, as mentioned before, to expressions with the same structure as those of model 2, so it is not possible on the basis of the present results to distinguish between models 2 and 3. We have plotted the present experimental kinetic results and also the results corresponding to zero CO_2 pressure from the work of Tøttrup (20), in accordance with Eqs. [10] and [11]; i.e., we have plotted $(P_{CO}/r_C)^{1/2}$ and $P_{CO}/r_C^{1/2}$ versus P_{CO}, in order to see if we can exclude one of the models as a possible mechanism. We have also plotted the results of Tøttrup (20) corresponding to a constant CO_2 pressure of 0.2 atm at 573 K. The results are summarized in Table 4. It was only possible to obtain a reasonable fit to the results obtained with CO_2 in the gas phase by using model 1. The results also clearly show, however, that when the gas does not contain CO_2 model 2 gives a much better description of the results than model 1. Values for the equilibrium constant K_A determined from the fits are shown in Table 4. The chemisorption of CO on nickel is probably the most thoroughly investigated chemisorption system. It is therefore possible, at least for clean and perfect nickel surfaces, to calculate reliable values for K_A by calculating the partition functions of gaseous and chemisorbed CO because the chemisorption energy and the vibrational frequencies are known. For each temperature, two theoretical values for K_A have been calculated by using the known value of the chemisorption energy of CO (109 kJ/mol (28)) and the vibrational frequencies of chemisorbed CO on Ni(100), in an on-top and in a bridge position, respectively, as calculated by Hähner et al. (29) in excellent agreement with available experimental results. The energy values used for calculating K_A are shown in Table 5. In comparing these theoretical K_A values with the ones from the fits it should be borne in mind, however, that by changing the chemisorption energy by as little as 10 kJ/mol, the value of K_A is changed by a factor of 6–8. The highest initial chemisorption energy reported for CO on nickel single crystals is 125 kJ/mol (30), while the value we have used is the value determined

TABLE 4

Experimental Results Fitted to Models 1 and 2

Ref.	Cat.	P_{CO_2} (atm)	T (K)	K_A model 1	K_A model 2	K_A theory	Best model
23	Ni	0.2	573	3.1	—	506–586	1
23	Ni	0	593	0.9	9.8	239–240	2
23	Ni	0	613	2.6	31.2	118–120	2
p.w.[a]	Ni	0	653	0.9[b]	10.1	33–36	2
p.w.[a]	$Cu_{0.1}$[c]	0	693	0.8[b]	9.4	11–12	2
p.w.[a]	$Cu_{0.1}$[c]	0	713	0.5[b]	6.4	6–11	2

[a] Present work.
[b] Bad fit.
[c] $Ni_{0.9}Cu_{0.1}$.

TABLE 5

Energies Used for Calculating Partition Functions

Species	Vibrational energies (J/mol)	Degeneracy	Bond energy (kJ/mol)
CO on Ni(100)			109
Bridge site	23052.9	1	
	4279.3	1	
	2662.3	1	
	7931.9	1	
	3287.8	1	
	446.1	1	
On-top Site	24757.2	1	
	5743.2	1	
	4553.2	2	
	413.8	2	

	Vibrational energy (J/mol)	Degeneracy	Enthalpy of formation at 298.15 K	Rotational constant (J/mol)	Symmetry number
CO (gas)	25953.0	1	−110.5	23.09	1

TABLE 6

Fit Parameters for 20 kPa Results for Ni/SiO_2

Model	k_0	E_k (kJ/mol)	E_{CO^*} kJ/mol
1 bridge CO	9.96×10^6	71.1	104.4
1 on-top CO	1.00×10^7	71.4	95.0
2 bridge CO	7.97×10^{15}	178.0	103.8
2 on-top CO	7.95×10^{15}	176.8	93.5

by temperature programmed desorption (28), which we believe is a more realistic value to use in the present case. It is remarkable that two of the fits with a reasonable number of points for Ni catalysts (613 K and 653 K runs) gives K_A values in good agreement with the calculated values for the bridge position chemisorption, while the results for the NiCu catalysts are in somewhat better agreement with the results for the on-top position. It is also interesting to note that the fits give a much smaller value than the theoretical one when the gas contains CO_2. The results lead us to suggest that the presence of CO_2 in the gas gives oxygen on the surface via step [6]. The oxygen diminishes the stability of CO preventing step [8] and enhancing step [6] thus forcing the mechanism of model 1 to dominate, while when CO_2 is absent the mechanism of model 2 dominates. Of course, in general, both mechanisms will contribute, but with the limited experimental data available we are not able in the modelling to go beyond the "one mechanism" approximation.

More complete tests of models 1 and 2 on our experimental results are provided by comparing model rates, calculated by using the theoretical equilibrium constant for CO chemisorption and a rate constant of Arrhenius form, with all the experimental rates covering a wide range of temperatures (593–713 K) and CO pressures (10–30 kPa). Arrhenius plots of most of the experimental rates obtained for the Ni/SiO_2 catalyst together with curves representing model rates are shown in Figs. 4 and 6, for models 2 and 1, respectively. The preexponential factor and the activation energy of the rate constant, as well as a "best" value for the chemisorption energy of CO, have been determined by adjusting their values to obtain the best fit to the 12 experimental rates measured for $P_{CO} = 20$ kPa at temperatures below 680 K. The values obtained for the rate constant and the chemisorption energy are shown for models 1 and 2 in Table 6. The chemisorption energy obtained for bridge-bonded CO is about 104 kJ/mol in excellent agreement with the chemisorption energy determined by Vink *et al.* (31) for CO adsorbed on Ni(111) with predeposited carbon. It is seen that model 1 as well as model 2 give excellent agreement with the

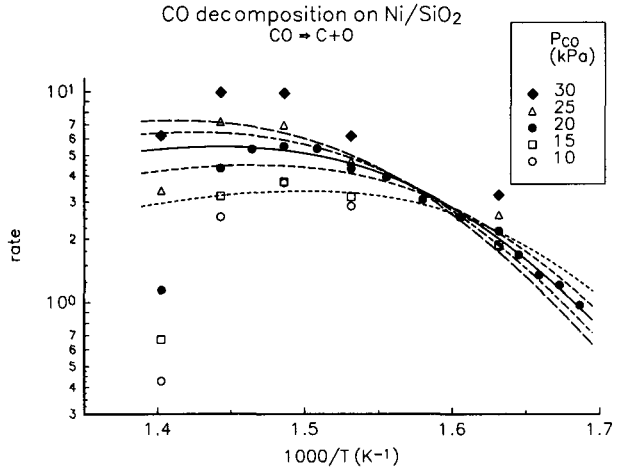

FIG. 6. Same experimental points as in Fig. 4, but the lines are calculated using the kinetic model 1.

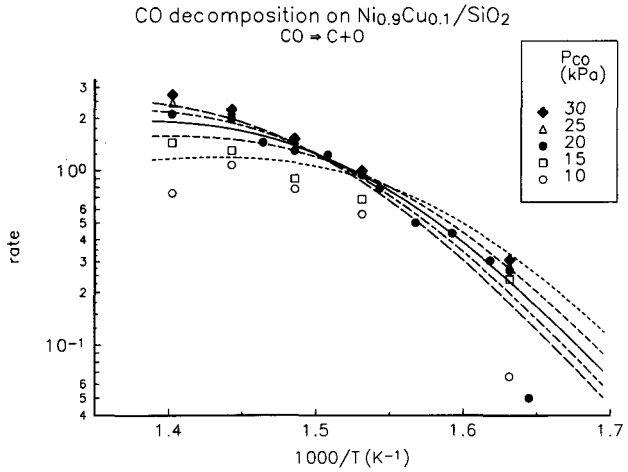

FIG. 7. Same experimental points as in Fig. 5, but the lines are calculated using the kinetic model 1.

TABLE 7

Fit Parameters for 20 kPa results for $Ni_{0.9}Cu_{0.1}/SiO_2$

Model	k_0	E_k (kJ/mol)	E_{CO^*} kJ/mol
1 bridge CO	3.10×10^6	73.9	109.4
1 on-top CO	3.10×10^6	73.9	99.7
2 bridge CO	9.34×10^{15}	169.8	110.7
2 on-top CO	9.28×10^{15}	168.7	99.9

experimental rates at $P_{CO} = 20$ kPa and temperatures below 680 K. At higher temperatures the experimental rates drop down far more rapidly with increasing temperature than the model rates. This is most likely to be due to poisoning of the catalyst by the formation of graphitic carbon, which does not disappear from the surface by migration through the nickel particle and segregation into the carbon filament. Also diffusion restrictions due to the formation of large amounts of carbon may contribute to the drop. The model rate curves in Fig. 4 show that model 2 gives good agreement with the experimental results with the exception of results obtained at the lowest CO pressure (10 kPa). The pressure dependence of the model 1 results are seen in Fig. 6 to be qualitatively wrong at the lower temperatures. The experimental $P_{CO} = 10$ kPa results are close to the $P_{CO} = 15$ kPa results and much higher than the model 2 results. Thus the results suggest that at CO pressures above 10 kPa the mechanism of model 2 dominates while the one of model 1 may contribute significantly at lower CO pressures.

Model 2 and model 1 have in the same way been tested on the experimental rates obtained for the $Ni_{0.9}Cu_{0.1}/SiO_2$ catalyst. The results are shown in Figs. 5 and 7. The "best" values obtained for the preexponential factor and the activation energy of the rate constant and for the

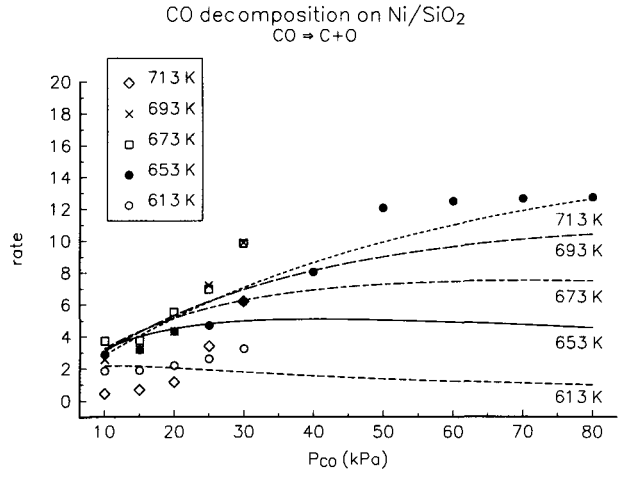

FIG. 8. Same experimental points as in Fig. 2, but the lines are calculated using the kinetic model 1.

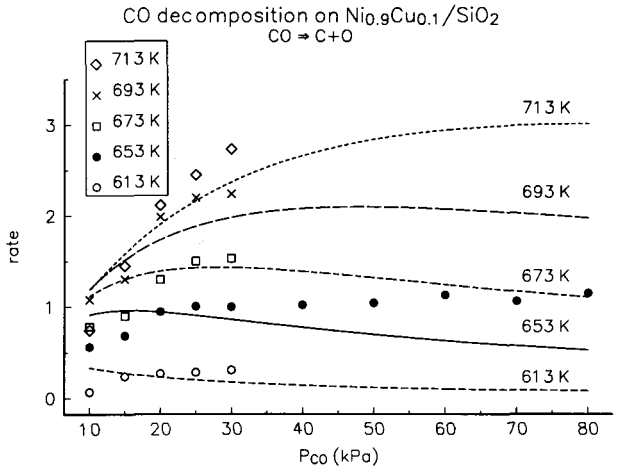

FIG. 9. Same experimental points as in Fig. 3, but the lines are calculated using the kinetic model 1.

chemisorption energy of CO are shown in Table 7. In this case, the bridge-bonded CO chemisorption energy obtained from the fit is close to the value for the clean nickel surface. It is seen that model 2 gives good agreement with the experimental rates also for the alloy catalyst while the model 1 results are qualitatively wrong also in this case. The experimental rates measured for Ni/SiO_2 have been plotted versus CO pressure and compared with model 2 and 1 rates in Figs. 2 and 8, respectively. It is seen that in a limited CO pressure range, 15–50 kPa, model 2 gives a satisfactory description of the results while model 1 results show a qualitatively wrong behavior. At CO pressures higher than 50 kPa the experimental rates do not follow the same increase as the model 2 rates but stay almost constant. Again this deviation may be due to graphitic poisoning of the nickel surface and to diffusion restrictions at the high decomposition rates. Very similar results are obtained for the alloy catalyst as seen in Figs. 3 and 9.

5. CONCLUSIONS

It is shown that carbon formation and gasification on nickel and nickel–copper catalysts in $CO + CO_2$ gas mixtures are reversible processes so that at zero rate all steps of the process are at equilibrium.

ΔG_C, the deviation of the free energy of carbon formation in $CO + CO_2$ gas mixtures from graphite equilibrium, is at equilibrium the same for nickel and for nickel–copper catalysts if the copper content is equal to or less than 25 at.% of the total metal content.

The deviation from graphite equilibrium is higher for nickel and nickel–copper catalysts in $CO + CO_2$ than for the same catalysts in $CH_4 + H_2$ gas mixtures.

The kinetic results for carbon formation on nickel and nickel–copper catalysts in pure CO at temperatures below

about 680 K and at CO pressures in the range 15–50 kPa are well described by a model in which the rate-limiting step is the reaction of two CO molecules adsorbed on the nickel surface with a carbon atom and a carbon dioxide molecule as products. At low CO pressures and when CO_2 is present in the gas the kinetic results are better described by a model in which the rate-limiting step is dissociation of CO on the surface.

ACKNOWLEDGMENTS

Part of this work has been supported by the Danish Research Councils through the Center for Surface Reactivity. The visits of M. T. Tavares to the Haldor Topsøe Research Laboratories were supported within the COMETT Programme 89/4/2051 Bb.

REFERENCES

1. Rostrup-Nielsen, J. R., *in* "Catalysis, Science and Technology" (J. R. Anderson and M. Boudart, Eds.), Vol. 5, Chap. 1. Springer-Verlag, Berlin 1984.
2. Rostrup-Nielsen, J. R., *J. Catal.* **85,** 31 (1984).
3. Bernardo, C. A., Alstrup, I., and Rostrup-Nielsen, J. R., *J. Catal.* **96,** 517 (1985).
4. Dent, F. J., and Cobb, J. W., *J. Chem. Soc.* **2,** 1903 (1929).
5. Rostrup-Nielsen, J. R., *J. Catal.* **27,** 343 (1972).
6. Lobo, L. S., Trimm, D. L., and Figueiredo, J. L., *in* "Proceedings, 5th International Congress on Catalysis, Florida, 1972" (J. W. Hightower, Ed.), p. 1125. North-Holland, Amsterdam 1973.
7. Baker, R. T. K., Barber, M. A., Harris, P. S., Feates, F. S., and Waite, R. J., *J. Catal.* **26,** 51 (1972).
8. Manning, M. P., Garmirian, J. E., and Reid, R. C., *Ind. Eng. Chem. Process Des. Dev.* **21,** 404 (1982).
9. De Bokx, P. K., Kock, A. J. H. M., Boellaard, E., Klop, W., and Geus, J. W., *J. Catal.* **96,** 454 (1985).
10. Kock, A. J. H. M., de Bokx, P. K., Boellaard, E., Klop, W., and Geus, J. W., *J. Catal.* **96,** 468 (1985).
11. Boellaard, E., de Bokx, P. K., Kock, A. J. H. M., and Geus, J. W., *J. Catal.* **96,** 481 (1985).
12. Alstrup, I., *J. Catal.* **109,** 241 (1988).
13. Grabke, H. J., *Metall. Trans.* **1,** 2972 (1970).
14. Lázár, K., Kertész, K. Császár-Gilicze, É., and Konczos, G., *Z. Metallkd.* **71,** 124 (1980).
15. Alstrup, I., and Tavares, M. T., *J. Catal.* **139,** 513 (1993).
16. Alstrup, I., and Tavares, M. T., *J. Catal.* **135,** 147 (1992).
17. Audier, M., and Coulon, M., *Carbon* **23,** 317 (1985).
18. Bianchini, E. C., and Lund, C. R. F., *J. Catal.* **117,** 455 (1989).
19. Safvi, S. A., Bianchini, E. C., and Lund, C. R. F., *Carbon* **29,** 1245 (1991).
20. Tøttrup, P. B., *J. Catal.* **42,** 29 (1976).
21. Rosei, R., Ciccacci, F., Memeo, R., Mariani, C., Caputi, L. S. Papagno, L., *J. Catal.* **83,** 19 (1983).
22. Kuijpers, E. G. M., Kock, A. J. H. M., Nieuwesteeg, M. W. C. M. A., and Geus, J. W., *J. Catal.* **95,** 13 (1985).
23. Sakai, N., Chida, T., Tadaki, T., and Shimoiizaka, J., *J. Chem. Eng. Japan* **18,** 199 (1985).
24. Kjær, J., "Computer Methods in Gas Phase Thermodynamics," Haldor Topsøe, Vedbæk 1972.
25. Turkdogan, E. T., Physical Chemistry of High Temperature Technology, Academic Press, New York, 1980.
26. Tracz, E., Scholz, R., and Borowiecki, T., *Appl. Catal.* **66,** 133 (1990).
27. Sørensen, O., Tavares, M. T., and Alstrup, I., unpublished.
28. Yates, J. T., and Goodman, D. W., *J. Chem. Phys.* **73,** 5371 (1980).
29. Hähner, G., Toennies, J. P., and Wöll, Ch., *Appl. Phys. A* **51,** 208 (1990).
30. Christmann, K., Schober, O., and Ertl, G., *J. Chem. Phys.* **60,** 4719 (1974).
31. Vink, T. J., van Zandvoort, M. M. J., Gijzeman, O. L. J., and Geus, J. W., *Appl. Surf. Sci.* **18,** 255 (1984).